Microstrip Line Negative Group Delay Filters for Microwave Circuits

Girdhari Chaudhary, *Member, IEEE*, Yongchae Jeong, *Senior Member, IEEE*, and Jongsik Lim, *Senior Member, IEEE*

***Abstract*—This paper presents a novel approach to the design and implementation of a distributed transmission line negative group delay filter (NGDF) with a predefined negative group delay (NGD) time. The newly proposed filter is based on a simple frequency transformation from a low-pass filter to a bandstop filter. The NGD time can be purely controlled by the resistors inserted into the resonators. The performance degradation of the NGD time and signal attenuation (SA) of the proposed NGDF according to the temperature dependent resistance variation is also analyzed. From this analysis, it is shown that the NGD time and SA variations are less sensitive to the resistance variation compared to those of the conventional NGD circuit. For an experimental validation of the proposed NGDF, a two-stage distributed microstrip line NGDF is designed, simulated, and measured at an operating center frequency of 1.962 GHz. These results show a group delay time of −7.3 ns with an SA of 22.65 dB at the center frequency and have good agreement with the simulations. The cascaded response of two NGDFs operating at different center frequencies is also presented in order to obtain broader NGD bandwidth. NGDFs with good reflection characteristics at the operating frequencies are also designed and experimentally verified.**

***Index Terms*—Bandstop filter (BSF), distributed transmission line, frequency transformation, negative group delay filter (NGDF), signal attenuation (SA).**

I. Introduction

In RECENT years, a physical phenomenon referred to as negative group delay (NGD) or superluminal wave propagation [1] has been implemented in electronic circuitry and applied to various practical applications in communication systems, such as shortening or reducing delay lines, efficiency enhancement of a feedforward linear amplifier, bandwidth (BW) enhancement of a feedback linear amplifier, and beam-squint minimization in phased array antenna systems [2]–[7]. These NGD phenomena can be observed within the limited frequency band of signal attenuation (SA) in certain media where higher frequency components of applied waveforms are propagated with phase advancement, not delay, relative to the lower frequency components [8], [9]. The group delay (GD) characteristics in circuit can be investigated by examining phase (φ) variation of forward transmitting scattering parameter. Using the differential-phase GD (τ_g) relation,

$$\tau_g = -\frac{d\varphi}{d\omega} \tag{1}$$

the presence of NGD in circuit is equivalent to an increasing phase (positive slope) with frequency.

Since the NGD synthesizer operating at a microwave frequency was presented in [10] and [11] , various active/passive NGD circuits have been designed in previous works using *RLC* resonators [12]–[20] and artificial media [21], such as left handed-metamaterial (LHM). However, the designed circuits were based on the single resonator concept [10]–[20] and the higher order filter synthesis methods were not discussed in these works. Moreover, these circuits suffered from smaller NGD-BW products and excessive SA.

Microwave/RF filters such as bandstop filters (BSFs) are key building blocks of modern RF communication systems, as they are used to filter out undesired signals because of their SA characteristics. Various approaches have been applied to design different kinds of BSFs [22]–[28]. However, these works have only focused on designing BSFs with large attenuation at specific stopband and cannot provide the predefined amount of NGD value. Moreover, no prior works have utilized the SA characteristics of BSFs to investigate NGD behavior.

In this paper, a distributed transmission line negative group delay filter (NGDF) topology with a predefined NGD time is presented for the first time, to the authors' best knowledge. The newly proposed filter utilizes the SA characteristic of a BSF to investigate the NGD phenomena. The circuit element values of the proposed NGDF are easily obtained by applying a frequency transformation from the Butterworth type low-pass filter (LPF) prototypes to the BSF, and the required NGD time is obtained by inserting resistors into the resonators. From the analysis, it is found that the proposed NGDF is less sensitive to temperature variations.

This paper is organized as follows. First, the theory and design equations of the NGDF are discussed to determine the element values of the filter from the specification of an NGDF in Section II. The performance degradation and implementation of the proposed NGDF with the distributed transmission line are also discussed in this section. Secondly, the simulation and measurement results are described in Section III, followed by the conclusion in Section IV.

Manuscript received August 08, 2013; revised December 04, 2013; accepted December 09, 2013. Date of publication January 02, 2014; date of current version February 03, 2014. This work was supported by the National Research Foundation of Korea (NRF) under the Ministry of Education, Science, and Technology Basic Science Research Program (2013006660).

G. Chaudhary and Y. Jeong are with the Division of Electronics Engineering, Information Technology (IT) Convergence Research Center, Chonbuk National University, Jollabuk-do 561-756, Korea (e-mail: ycjeong@jbnu.ac.kr).

J. Lim is with the Department of Electrical Engineering, Soonchunhyang University, Chungcheongnam-do 336-745, Korea.

Color versions of one or more of the figures in this paper are available online at http://ieeexplore.ieee.org.

Digital Object Identifier 10.1109/TMTT.2013.2295555

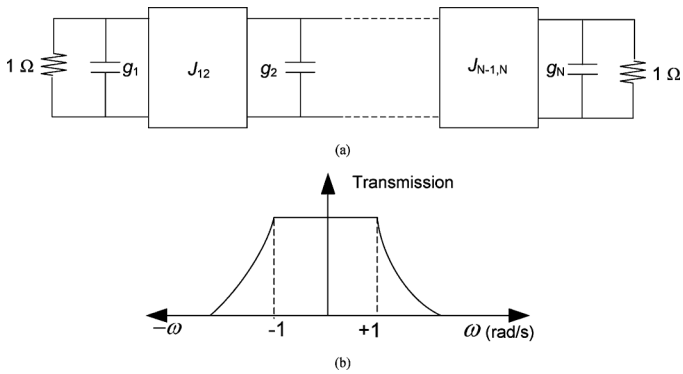

Fig. 1. (a) Butterworth LPF prototype network using J-inverters and (b) its frequency response.

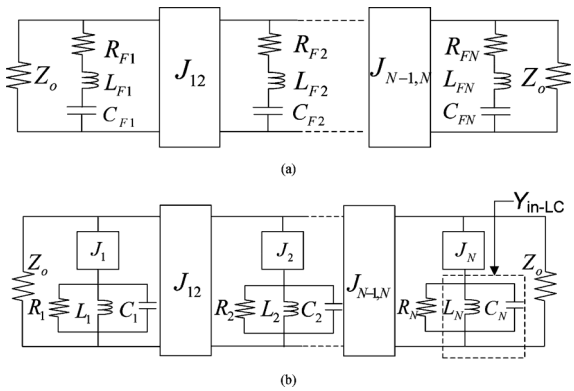

Fig. 2. Structures of NGDF. (a) Filter type I: J-inverters with series *RLC* resonators and (b) filter type II: J-inverters with parallel *RLC* resonators.

II. Theory and Design Equations

A. General Design Equations

Fig. 1 shows the J-inverter-coupled Butterworth LPF prototype network and its associated frequency response. The element values of this circuit [27] are obtained as follows:

$$J_{r,r+1} = 1 \tag{2a}$$

$$g_r = 2\sin\left[\frac{(2r-1)\pi}{2N}\right] \tag{2b}$$

$$r = 1, \ldots, N \tag{2c}$$

where N is the number of filter stages. This network can be transformed to the NGDF prototype shown in Fig. 2(a) by simply applying the following transformation equation and inserting resistors in the shunt resonators [27], [28]:

$$\frac{1}{\omega'} = \frac{1}{\Delta}\left(\frac{\omega}{\omega_0} - \frac{\omega_0}{\omega}\right) \tag{3}$$

where Δ and ω_0 are the 3-dB fractional bandwidth (FBW) and the angular center frequency of the NGDF, respectively.

Therefore, the element values of the NGDF shown in Fig. 2(a) can be calculated in (4) and (5) as follows:

$$C_{Fr} = \frac{\Delta g_r}{\omega_0 Z_0} \tag{4}$$

$$L_{Fr} = \frac{Z_0}{\omega_0 \Delta g_r}. \tag{5}$$

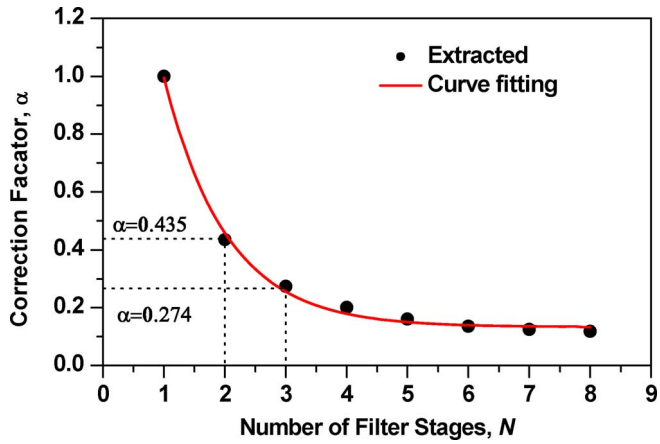

Fig. 3. Relationship between correction factor and number of filter stages.

The resistors are inserted into the shunt LC resonator to get the predefined NGD time. The resistances can be obtained by analyzing the shunt LC resonator, the values of which are given in (6) as follows:

$$R_{Fr} = -\frac{Z_0}{4} + \sqrt{\frac{Z_0^2}{16} - \frac{Z_0 L_{Fr}}{\alpha \tau_g}} \tag{6}$$

where Z_0, τ_g, and α are the terminated port impedance, GD time, and correction factor, respectively. The values of the admittance inverters ($J_{r,r+1}$) and r are the same as in (2a) and (2c), respectively. A correction factor (α) is inserted into (6) to take into account the fact that each resonator contributes to the GD time and increases the GD time so that it is higher than the required value for the overall circuit as N increases. To compensate for the deviation from the required value, α is inserted into (6) so that the exact value of the resistor can be obtained for the required NGD time. This value was obtained by comparing the exact resistance value for the required NGD time of the filter with the calculation using (6) with $\alpha = 1$, and is shown in Fig. 3. Using these extracted values, the expression of α is found as shown in (7) by using the nonlinear curve fitting method

$$\alpha = \alpha_0 + a_1 e^{-(N-b_0)/b_1} \tag{7}$$

where values of constants are given as $\alpha_0 = 0.13271$, $a_1 = 1.78864$, $b_0 = 0.25028$, and $b_1 = 1.02477$, respectively. For the design graph, the relationship between α and N is plotted in Fig. 3 and compared with extracted values for the validation. As seen in this figure, the curve fitted values are exactly matched with extracted values. As seen in this figure, as N increases, the value of α approaches toward the smaller value.

The NGDF prototype (filter type I) shown in Fig. 2(a) is not practically suitable for filter implementation due to the fact that the shunt series resonator branch results in physically unrealizable capacitance and inductance values so that it is not easy to realize with transmission lines. Therefore, the additional admittance inverters are inserted into the shunt branch to obtain the realizable component values by arbitrary scaling and can easily be implemented with the distributed elements. The values of

TABLE I
SPECIFICATON OF NGDFS

LPF prototype network	Filter stage (N)	LPF prototype elements values	Center frequency f_0 (GHz)	3-dB BW (MHz)	NGD τ_g (ns)
Butterworth	2	g_0=g_3=1.000 g_1=g_2=1.4142	1.962	200	-7
Butterworth	3	g_0=g_4=1.000 g_1=g_3=1.000 g_2=2.000	1.962	200	-7

TABLE II
ELEMENT VALUES OF UNMATCHED NGDF WITH $N = 2$

	Element values of Fig. 2(a)			Element values of Fig. 2(b)				
J_{12}	C_{F1}=C_{F2} (pF)	L_{F1}=L_{F2} (nH)	R_{F1}=R_{F2} (Ω)	J_{12}	J_1=J_2	C_1=C_2 (pF)	L_1=L_2 (nH)	R_1=R_2 (Ω)
1	0.2337	28.1453	12.3677	1	0.0083	1.9389	3.3923	1173.69

TABLE III
ELEMENT VALUES OF UNMATCHED NGDF WITH $N = 3$

Element values of Fig. 2(a)				Element values of Fig. 2(b)				
J_{12}	C_{F1}=C_{F3} (pF)	L_{F1}=L_{F3} (nH)	R_{F1}=R_{F3} (Ω)	J_{12}	J_1=J_2	C_1=C_3 (pF)	L_1=L_3 (nH)	R_1=R_3 (Ω)
1	0.1653	39.8031	22.0524	1	0.0083	2.7420	2.3994	658.25
J_{23}	C_{F2} (pF)	L_{F2} (nH)	R_{F2} (Ω)	J_{23}	J_3	C_2 (pF)	L_2 (nH)	R_2 (Ω)
1	0.3306	19.9015	13.4818	1	0.0083	1.3710	4.7989	1076.70

the modified NGDF (filter type II) shown in Fig. 2(b) are determined by equating the input admittance of the shunt resonators of Fig. 2(a) and (b).

Therefore, the closed-form element values for the NGDF shown in Fig. 2(b) are obtained as

$$L_r = \frac{C_{Fr}}{J_r^2} \tag{8}$$

$$C_r = L_{Fr} J_r^2 \tag{9}$$

$$R_r = \frac{1}{R_{Fr} J_r^2} \tag{10}$$

where J_r is a scaling factor admittance inverter and r is the same as in (2c). The values of J_r can be chosen arbitrarily so that physically realizable values of L_r and C_r can be obtained.

To validate the theoretical analysis, the NGDFs with specification defined in Table I are designed and simulated. The Butterworth-type LPF is considered in this work for its relatively flat GD characteristics. The values of α obtained from Fig. 3 are given as 0.435 for $N = 2$ and 0.274 for $N = 3$. The calculated element values of the NGDF for $N = 2$ and $N = 3$ are given in Tables II and III. As shown in Tables II and III, the lumped-element values (L_{Fr}, C_{Fr}) of Fig. 2(a) are not suitable for realization with microstrip lines. However, the realizable element values are obtained by introducing J_r, as shown in Fig. 2(b).

Fig. 4(a) shows the simulated GD and SA (S_{21}) characteristics of the proposed NGDF with $N = 2$ and is compared with

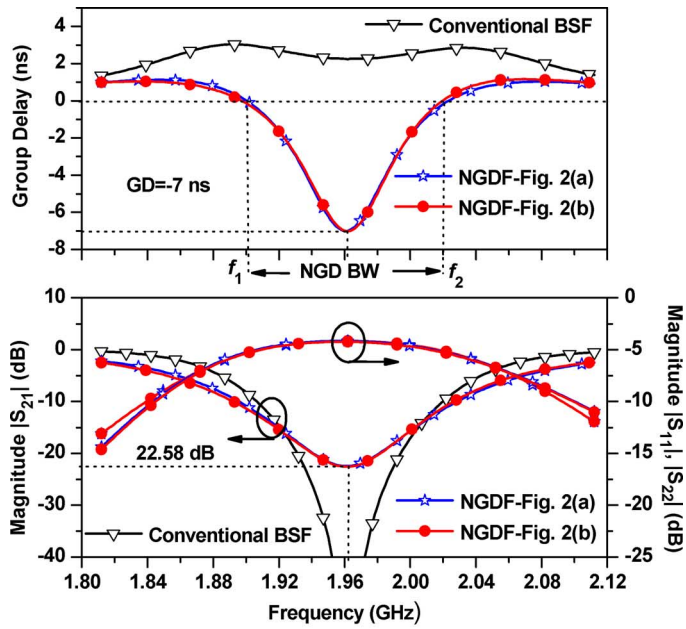

(a)

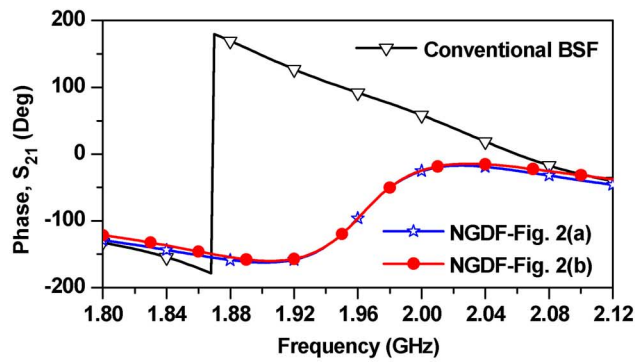

(b)

Fig. 4. Comparison results for conventional BSF and NGDF with $N = 2$. (a) GD/magnitude characteristics and (b) phase characteristics of S_{21}.

the conventional BSF. As shown in this figure, the GD time of -7 ns and the SA of 22.58 dB were obtained at $f_0 = 1.962$ GHz in case of the proposed NGDF, which can be compensated with a general purpose gain amplifier. Therefore, the SA value should be as small as possible, which helps to reduce gain burden of the amplifier as well as out-of-band noise and can provide a stable operation when the NGDF is integrated with an RF system [20]. The NGD-BW (NGD BW $= f_2 - f_1$) is defined as the BW of GD of 0 ns, as shown in Fig. 4 for convenience, and is generally slightly smaller than 3-dB BW. The NGD-BW of the proposed filter, as shown in Fig. 4(a), is 125 MHz, which is slightly less than the 3-dB BW.

The phase characteristics of the proposed NGDF and conventional BSF are shown in Fig. 4(b). As seen from this figure, the phase of S_{21} is increasing with frequency (positive slope) in the case of the NGDF, which signifies the presence of NGD, whereas it is decreasing with frequency (negative phase slope), which signifies positive GD in the case of the conventional BSF.

Fig. 5 shows the comparison of the GDs and the SA characteristics of the proposed filter for the different number of filter

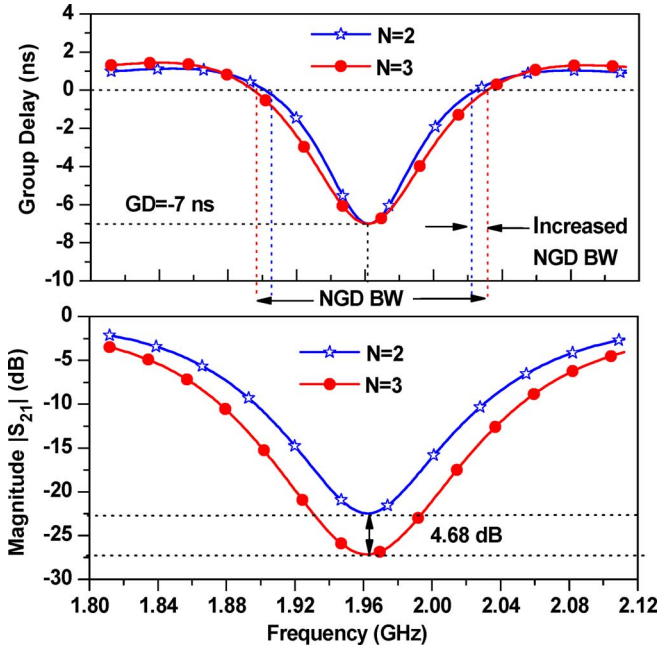

Fig. 5. Comparison of GDs and magnitude S_{21} characteristics for different number of filter stages.

stages. As shown in the figure, the NGD-BW is slightly increased as N increases. However, the SA is also increased for the same amount of GD time. Therefore, there are tradeoffs between the NGD time, SA, NGD-BW, and number of filter stages N.

B. Performance Degradation Analysis

The temperature dependence of a resistor is represented by the following relationship:

$$\frac{\Delta R}{R_0} = \delta \Delta T \tag{11}$$

where δ, R_0, ΔR, and ΔT are the temperature coefficient, initial resistance, resistance variation, and temperature variation, respectively.

Fig. 6 shows the performance degradation of the NGDF for the different values of N assuming the resistance variation of $\pm 5\%$. As seen from these figures, the GD time and SA variations are around ± 0.9 ns and ± 1.9 dB, respectively, from the reference values. However, the SA and NGD of the conventional NGD circuit varied significantly up to 22 dB and over 40 ns, respectively, with the same resistance variation [19]. Therefore, from these results, it is concluded that the proposed NGDF is considerably less sensitive to temperature-dependent resistance variations.

C. Distributed Transmission Line Implementation

A quarter-wavelength ($\lambda/4$) transmission line is one example of a practical J-inverter. The equivalence between the $\lambda/4$ transmission line and the J-inverter is obtained by equating the $ABCD$ parameters of both circuits [26]. Thus, the J-inverters are implemented with $\lambda/4$ microstrip lines in this work, as shown in Fig. 7. It can be observed that both load admittance

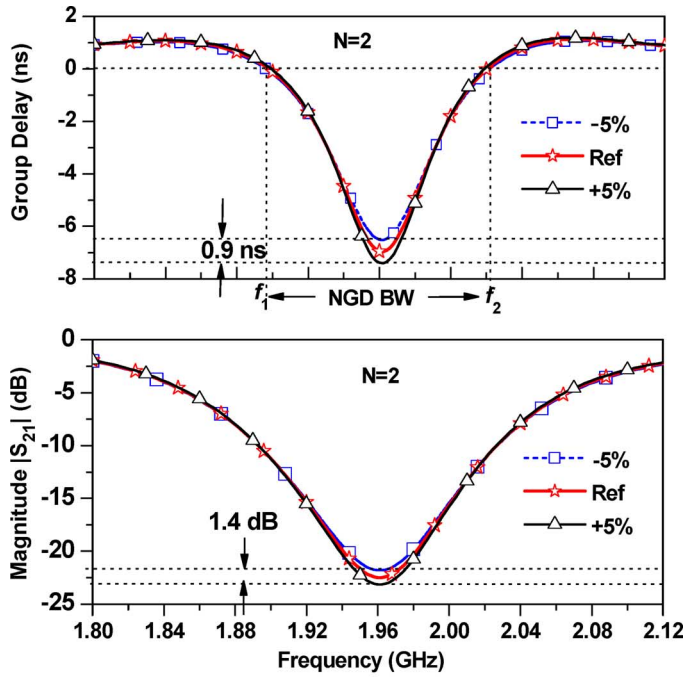

(a)

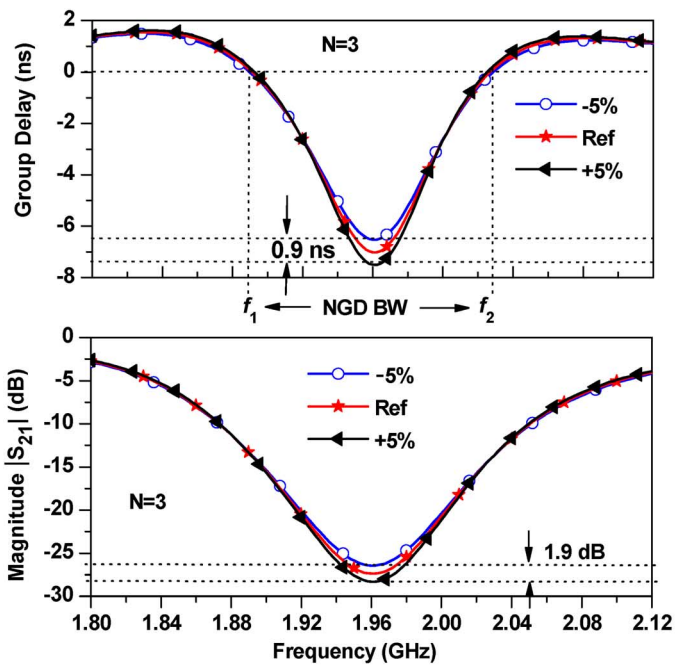

(b)

Fig. 6. Performance degradations of NGDF with resistance variation of 5% for different filter stages: (a) $N = 2$ and (b) $N = 3$.

functions (12) and (13) of the shunt parallel LC resonator and the short-circuited $\lambda/4$ transmission line from Figs. 2(b) and 7, respectively, have the same characteristics in the vicinity of $\omega = \omega_0$,

$$Y_{\text{in}-LC} = j\omega_0 C\left(\frac{\omega}{\omega_0} - \frac{\omega_0}{\omega}\right) \approx \pm j2C\Delta\omega \tag{12}$$

$$Y_{\text{in}-TLN} = j\frac{\pi}{4Z_N}\left(\frac{\omega}{\omega_0} - \frac{\omega_0}{\omega}\right) \approx \pm j\frac{\pi\Delta\omega}{2Z_N\omega_0} \tag{13}$$

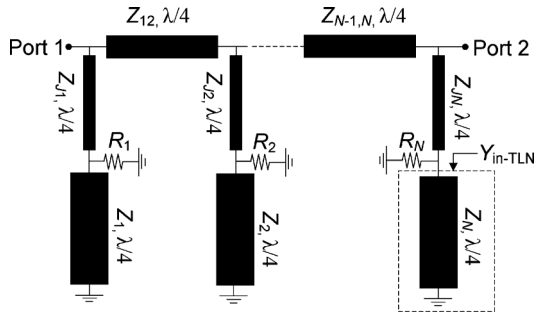

Fig. 7. Structure of distributed transmission line NGDF.

TABLE IV
ELEMENT VALUES OF TRANSMISSION LINE UNMATCHED NGDF [REFER TO FIG. 7]

N	Z_{12} (Ω)	Z_{J1}=Z_{J2}(Ω)	Z_1=Z_2 (Ω)	R_1=R_2 (Ω)
2	50	100	22.64	660.8

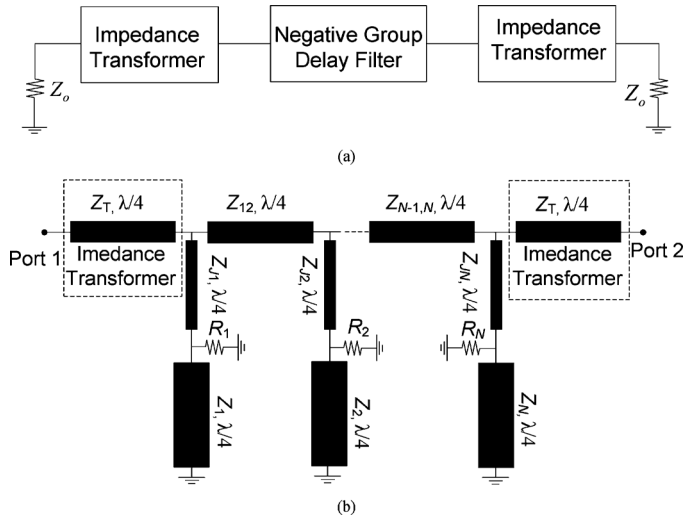

Fig. 8. Structure of matched NGDF. (a) General block diagram and (b) matched distributed transmission line NGDF.

where $\omega = \omega_0 \pm \Delta\omega$ and Z_N is the characteristic impedance of the transmission line. Therefore, the parallel LC resonators can be implemented with the short-circuited transmission line with the characteristic impedance Z_N and a physical length of $\lambda/4$ at ω_0. The element values of the unmatched transmission line NGDF designed for τ_g of -6.5 ns at f_0 of 1.962 GHz with the 3-dB BW of 200 MHz are described in Table IV.

D. Matched NGDF

As shown in Fig. 4, the proposed NGDF suffers from poor reflection characteristics. One of the ways to improve the reflection characteristic is through a balanced NGDF structure. However, this structure increases the number of components (such as hybrid couples) and the overall size. Therefore, a simple solution is to insert the input and output impedance transformer networks on both sides of the NGDF, as shown in Fig. 8. The purpose of impedance transformer networks is to transform the input/output impedances of the NGDF to the port impedance of 50 Ω. Since the structure is symmetrical, even- and odd-mode analysis can be applied to determine the required value of the characteristic impedance Z_T of impedance transformers. The S-parameters of the proposed structure of the matched NGDF can be obtained as follows in (14):

$$S_{11} = S_{22} = \frac{Z_{ine}Z_{ino} - Z_0^2}{(Z_{ine} + Z_0)(Z_{ino} + Z_0)} \tag{14a}$$

$$S_{21} = S_{12} = \frac{Z_{ine}Z_0 - Z_{ino}Z_0}{(Z_{ine} + Z_0)(Z_{ino} + Z_0)} \tag{14b}$$

where Z_{ine} and Z_{ino} denote the even-and odd-mode impedances, respectively, of the N-stage NGDF. For example, for $N = 2$, the impedances can be obtained as follows in (15):

$$Z_{ine} = \frac{Z_T + jZ_T^2 Y_{L1}\tan\beta l}{Z_T Y_{L1} + j\tan\beta l} \tag{15a}$$

$$Z_{ino} = \frac{Z_T + jZ_T^2 Y_{L2}\tan\beta l}{Z_T Y_{L2} + j\tan\beta l} \tag{15b}$$

where β and l are the propagation constant and length of the transmission line, respectively. The value of Y_{L1} and Y_{L2} are given as follows in (16):

$$Y_{L1} = \frac{Z_{J1}Z_1\tan\beta l - jZ_{J1}R_1 + jR_1Z_1\tan^2\beta l}{Z_{J1}R_1Z_1\tan\beta l + jZ_{J1}^2Z_1\tan^2\beta l + Z_{J1}^2R_1\tan\beta l} + j\frac{\tan\frac{\beta l}{2}}{Z_{12}} \tag{16a}$$

$$Y_{L2} = \frac{Z_{J1}Z_1\tan\beta l - jZ_{J1}R_1 + jR_1Z_1\tan^2\beta l}{Z_{J1}R_1Z_1\tan\beta l + jZ_{J1}^2Z_1\tan^2\beta l + Z_{J1}^2R_1\tan\beta l} - j\frac{1}{Z_{12}\tan\frac{\beta l}{2}}. \tag{16b}$$

For a matched network, it is required that S_{11} and S_{22} should be equal to zero. Assuming $l = \lambda/4$ at f_0, the required value of Z_T is obtained for the matched condition as follows in (17):

$$Z_T = \frac{Z_{J1}(Z_0Z_{12})^{1/2}}{(Z_{12}^2R_1^2 + Z_{J1}^4)^{1/4}}. \tag{17}$$

Furthermore, this design method can be applied to find the characteristic impedances of transformers for higher order filter stages.

Figs. 9 and 10 show the simulation results of the unmatched and matched NGDF, respectively, for the comparison. The element values of the matched NGDF are given in Table IV for the same design specification. To obtain the same GD time for both filters, the matched NGDF should be designed for a higher GD time than the required value because two impedance transformers provide a positive GD time. As shown in Fig. 10, the return losses of the matched NGDF are better than 50 dB at f_0. However, the NGD-BW of the matched NGDF is somewhat smaller than that of the unmatched NGDF due to the fact that the NGDF should be designed with a higher NGD time in order to compensate for the positive GD time of the impedance transformers. Designing the NGDF with a higher NGD time makes a narrow NGD-BW.

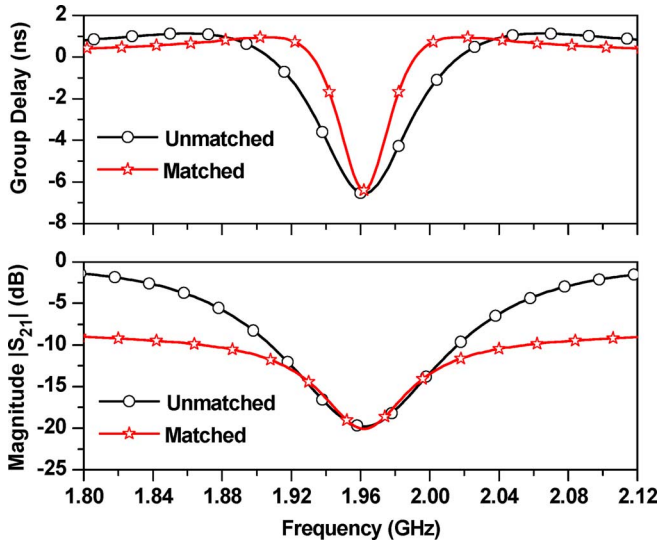

Fig. 9. Simulation results of matched and unmatched NGDF with $N = 2$.

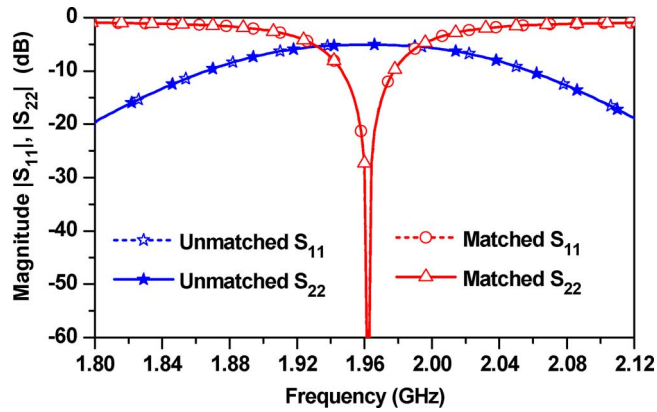

Fig. 10. Simulated return losses of matched and unmatched NGDF with $N = 2$.

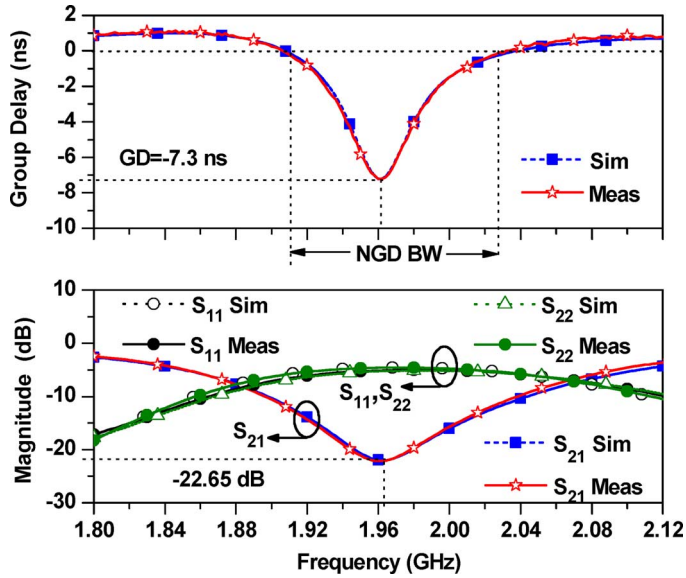

Fig. 11. Simulation and measurement results of unmatched NGDF with $N = 2$.

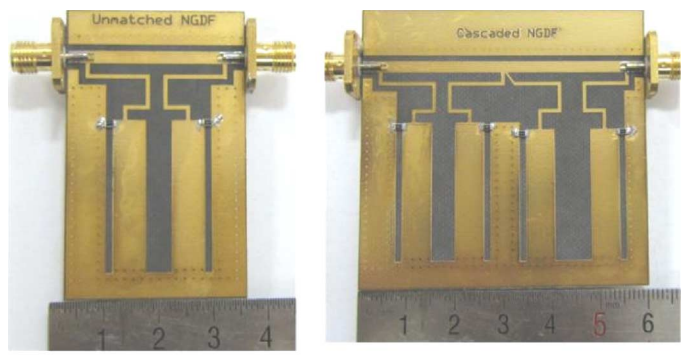

(a) (b)

Fig. 12. Photograph of fabricated NGDFs: (a) unmatched NGDF with $N = 2$ and (b) NGDF with two cascaded filters operating at two different center frequencies.

III. Implementation and Experimental Performance

To verify the design concept of the proposed NGDF, a two-stage filter ($N = 2$) with specification given in Table I is designed and fabricated for the US personal communication service (PCS) downlink center frequency (f_0) of 1.962 GHz. With the specification of the filter, the lumped element values of the NGDF shown in Fig. 2(b) are obtained as $J_{12} = J_{23} = 1$, $J_1 = J_2 = 0.01, C_1 = C_2 = 2.8153$ pF, $L_1 = L_2 = 2.337$ nH, and $R_1 = R_2 = 660.8\ \Omega$.

The element values of the unmatched distributed NGDF are given in Table IV. The filter is fabricated on substrate RT/Duroid 5880 from Rogers Inc. with a dielectric constant (ε_r) of 2.2 and a thickness (h) of 31 mil. To reduce the circuit size, J-inverters implemented with a $\lambda/4$ line are meandered. The simulation is performed using Ansoft's HFSS v13.

Fig. 11 shows the simulation and measurement results of the unmatched NGDF. From the measurements, it is determined that the GD time of -7.3 ns with an SA of 22.65 dB at 1.962 GHz are obtained and the NGD-BW is around 100 MHz, which is slightly less than 3-dB BW. As shown in Fig. 11, the measurement results are in good agreement with the simulations. Fig. 12(a) shows a photograph of fabricated circuit of unmatched NGDF.

A. Enhancement of NGD-BW

As shown by the results in the previous sections, the NGD-BW of the proposed filter is narrow. One of the ways to increase the NGD-BW is to increase N. However, increasing N cannot provide the large increase in the NGD-BW that is shown in Fig. 5. Another way to employ the NGDF with a broader NGD-BW is to cascade NGDFs operating at different center frequencies.

Fig. 13 shows the simulation and measurement results of two cascaded unmatched NGDFs. Fig. 13 also shows the simulation results of the fourth- and fifth-order NGDFs for comparison. In this work, the two units of NGDFs of the second order are designed for $f_1 = 1.940$ GHz and $f_2 = 1.984$ GHz, respectively, and are cascaded in order to get an NGD-BW of 200 MHz and a center frequency $f_0 = 1.962$ GHz. As seen from these figures, the measurement results of two cascaded

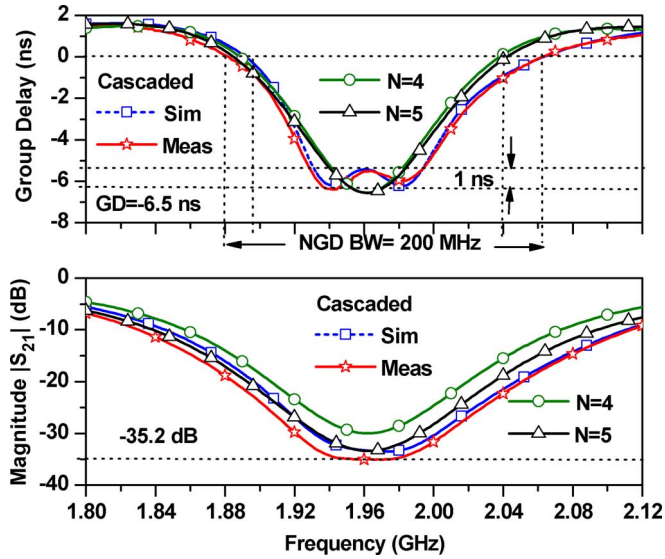

Fig. 13. Simulation and measurement results of unmatched NGDF with two cascaded filters operating at two different center frequencies.

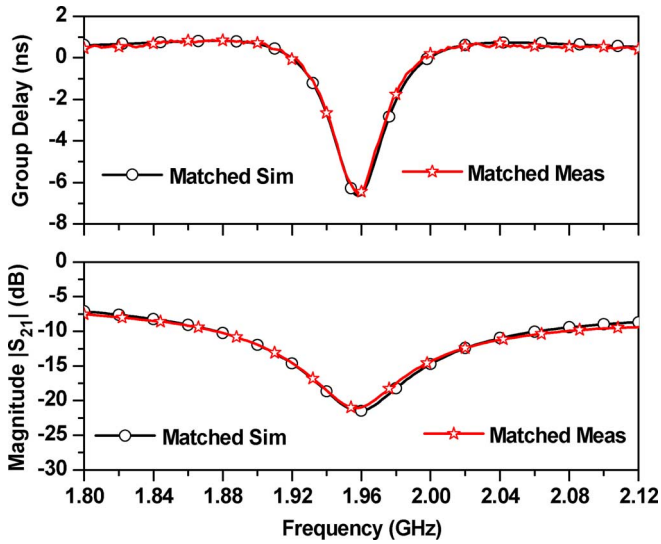

Fig. 14. Simulated and measured GD/magnitude S_{21} characteristics of matched NGDF with $N = 2$.

TABLE V
ELEMENT VALUES OF TRANSMISSION LINE MATCHED NGDF
[REFER TO FIG. 8(b)]

N	Z_{12} (Ω)	Z_{J1}=Z_{J2}(Ω)	Z_1=Z_2 (Ω)	R_1=R_2 (Ω)	Z_T (Ω)
2	50	100	22.64	980	22.58

NGDFs have good agreement with the simulations. From the measurements, a maximum achievable GD time of −6.5 ns with an SA of 35.2 dB are obtained. The measured NGD-BW of the cascaded NGDF is somewhat broader than those of the fourth- and fifth-order NGDF. A photograph of the fabricated cascading NGDF is shown in Fig. 12(b).

B. Matched NGDF

To validate the theoretical analysis of the NGDF with improved return losses, a two-stage microstrip matched NGDF was designed and measured. For this purpose, the filter is designed with the same specification given in Table I, except for $\tau_g = -7.5$ ns, which is some higher value than required value (−6.5 ns) in order to compensate positive GD time of impedance transformers. Therefore, the element values of the proposed matched NGDF with $N = 2$ are the same as the unmatched NGDF, except resistance values (R_1 and R_2), which are given in Table V.

Fig. 14 shows the simulated and measured GD and SA values of the matched NGDF. The simulation and measurement results of the matched NGDF have good agreement. As shown in these figures, a GD time of −6.5 ns is obtained with an SA (S_{21}) of 21.5 dB at 1.961 GHz. However, the NGD-BW of the matched NGDF is somewhat smaller than that of the unmatched NGDF due to the fact that the NGDF should be designed with a somewhat higher NGD time to compensate for the positive GD time of the impedance transformers.

Fig. 15 shows a return-loss characteristics of the matched NGDF. As shown in this figure, the return-loss characteristics

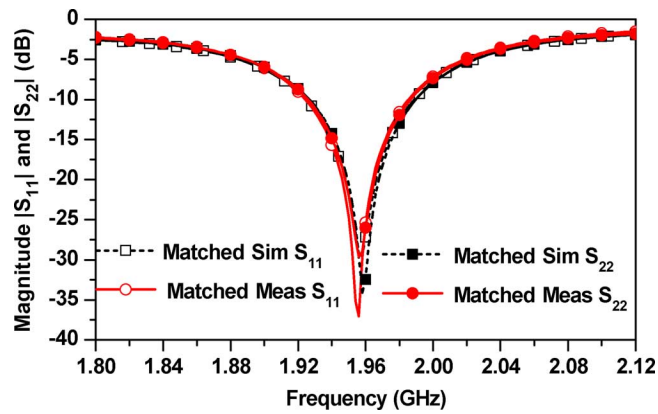

Fig. 15. Simulated and measured return loss of matched NGDF with $N = 2$.

of the matched NGDF are better than 24 dB at 1.961 GHz. The photograph of the fabricated matched NGDF is shown in Fig. 16.

The structure of the matched cascading NGDF with enhanced NGD-BW is shown in Fig. 17. In this structure, two NGDFs (NGDF_1 and NGDF_2) with $N = 2$ operating at different center frequencies (f_1 and $f_{2,}$) are cascaded. To obtain improved input/output return-loss characteristics, first input and output impedances (Z_{in1} and Z_{in2}) are calculated at $f_0 = (f_1 + f_2)/2$ without considering the open/short stubs. The values of Z_{in1} and Z_{in2} at f_0 are given as $R_{\mathrm{in1}} + jX_{\mathrm{in1}}$ and $R_{\mathrm{in2}} - jX_{\mathrm{in2},}$ respectively. Secondly, the open stub line with the characteristic impedance Z_{op} and electrical length θ_{op} is added to compensate the inductive reactance of Z_{in1} and obtaining a purely resistive $Z_{\mathrm{in1}} = R_{\mathrm{in1}}$. Similarly, to obtain a purely resistive $Z_{\mathrm{in2}} = R_{\mathrm{in2}}$ by compensating the capacitive reactance of Z_{in2}, the short stub with a characteristic impedance Z_{sc} and electrical length θ_{sc} is connected, as shown in Fig. 18. Lastly, the purely resistive values of R_{in1} and R_{in2} are transformed to Z_0 at f_0 using the $\lambda/4$ transmission lines. Further, this method can be extended for

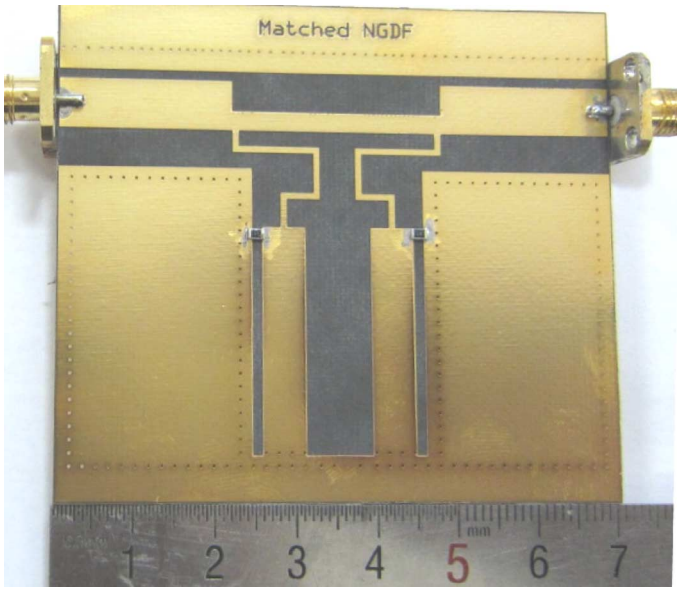

Fig. 16. Photograph of fabricated matched NGDF.

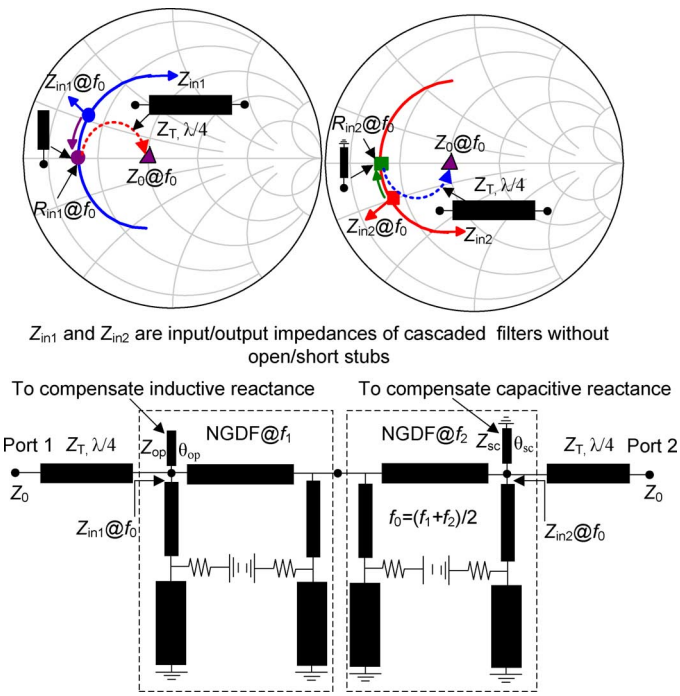

Fig. 17. Proposed structure of matched NGDF with two cascading filters operating at different center frequencies and its design method.

higher number (more than two) of cascading NGDFs to design the NGD time with multiple zeros for NGD-BW enhancement.

For the experimental validation of the proposed structure of the matched cascading NGDF, the goal was set as a τ_{gmax} of -6.5 ns at $f_0 = 1.962$ GHz and an NGD-BW of 200 MHz. For this purpose, NGDF_1 and NGDF_2 are designed at $f_1 = 1.940$ GHz and $f_2 = 1.984$ GHz, respectively. The circuit parameters of NGDF_1 and NGDF_2, shown in Fig. 17, are given in Table IV, except for the resistances. The characteristic impedances and the electrical lengths of the open and short stubs are given as $Z_{\mathrm{op}} = 34\ \Omega$, $\theta_{\mathrm{op}} = 36°$, and $Z_{\mathrm{sc}} = 80\ \Omega$, $\theta_{\mathrm{sc}} = 25°$,

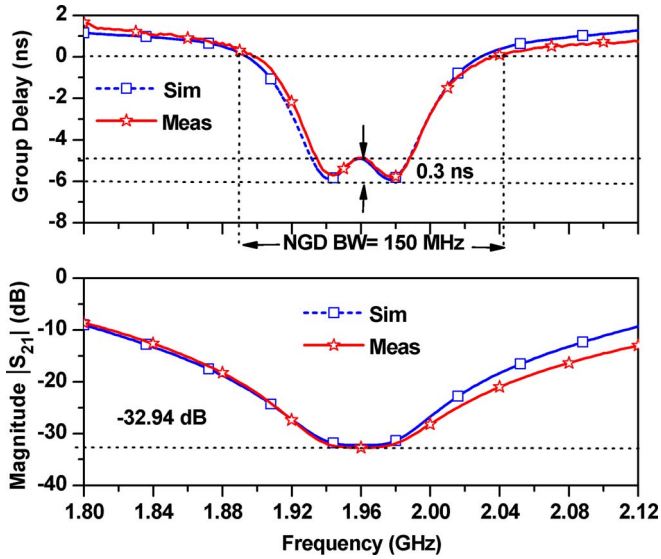

Fig. 18. Simulation and measurement results of matched NGDF with two cascading filters.

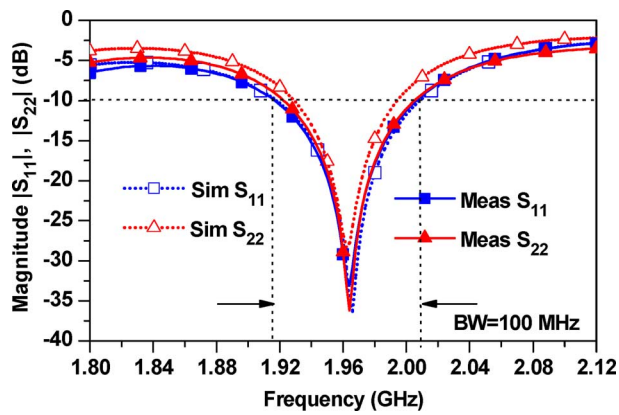

Fig. 19. Simulation and measurement results of matched NGDF with two cascading filters.

respectively, to compensate for the inductive/capacitive reactance of the input impedances. The characteristic impedances of the $\lambda/4$ transformers are given as 29.5 Ω in this work.

The simulation and measurement results of the matched cascading NGDF are shown in Fig. 18. The measured results have good agreement with the simulations results. As shown in these figures, the maximum achieved NGD is -6 ns with an SA of 32.94 dB and an NGD-BW of 150 MHz. However, the NGD-BW of this structure is slightly less than that of the unmatched cascading NGDF due to the positive GD of the open/short stubs and impedances transformers in the matched filter.

The simulated and measured input/output return losses of the matched cascading NGDF are shown in Fig. 19. As shown in this figure, the measurement results are in good agreement with the simulations. The input/output return losses (S_{11} and S_{22}) are better than 30 dB at $f_0 = 1.962$ GHz and 10 dB in the range of 1.91–2.01 GHz, respectively. Since the impedance matching is concentrated at f_0 only, the good return characteristics are obtained at this frequency. Moreover, the BW of return-loss characteristics is slightly smaller than NGD-BW, as shown in

TABLE VI
PERFORMANCE COMPARISON OF PROPOSED NGDF WITH OTHERS WORKS

	Center Frequency f_0 (GHz)	Circuit Type	Maximum Achieved NGD Time (ns)	NGD BW (MHz)	SA_{max} (dB)	NGD Time x BW Product
[3]	2.14	Passive	-9	30	-63	0.270
[10]	1	Active	-10	40	30	0.400
[11]	1	Active	-10	40	30	0.400
[12]	1	Active	-2.3	150	2.3	0.345
[15]	4.5	Passive	0.05	3000	-10	0.150
[17]	1.03	Active	-2.3	150	1.68	0.345
[19]	0.454	Active	-1.52	103	0.69	0.156
This Work^{I}	**1.962**	**Passive**	**-7.3**	**100**	**-22.65**	**0.730**
This Work^{II}	**1.962**	**Passive**	**-6.5**	**200**	**-35.2**	**1.300**
This Work^{III}	**1.962**	**Passive**	**-6.5**	**90**	**-21.20**	**0.585**
This Work^{IV}	**1.962**	**Passive**	**-6.0**	**150**	**-32.94**	**0.900**

SA_{max}: Maximum Signal Attenuation ($|S_{21}|$) at f_0
I : Unmatched NGDF with N=2
II: Unmatched NGDF with cascading two filters operating at different center frequencies
III : Matched NGDF with N=2
IV: Matched NGDF with cascading two filters operating at different center frequencies

Figs. 18 and 19, which is due to narrowband characteristics of impedance transformers [28]. However, it can be improved by utilizing wideband impedance transformers.

Table VI shows the performance comparison of the proposed NGDF among the previous works. Due to the tradeoff between the achieved NGD time and the BW, the appropriate parameter to compare the circuit's performance is the NGD-BW product. Therefore, as shown in this table, the proposed NGDFs provide improved NGD-BW products compared to the previous works.

IV. CONCLUSION

In this paper, the design and implementation of a distributed transmission line NGDF topology with a predefined GD time has been demonstrated. The NGD is obtained by inserting external resistors into the resonators of the BSF. The proposed NGDF is less sensitive to the temperature-dependent resistance variation. For the experimental validation, a second-order negative group filter with the predefined NGD was designed, simulated, and measured. The measurement results were in good agreement with the theoretical predictions. The design method for the NGDF with improved input/output return loss was also discussed and experimentally verified. To enhance the NGD-BW, the response of a cascaded two-stage NGDF operating at different frequencies was also presented in this paper. This design method and topology are also applicable to higher order NGDFs. The proposed filter topology is simple to implement and is expected to be applicable in various wireless communication systems.

REFERENCES

[1] L. Brillouin and A. Sommerfeld, *Wave Propagation and Group Velocity*. New York, NY, USA: Academic, 1960, pp. 113–137.
[2] M. Kitano, T. Nakanishi, and K. Sugiyama, "Negative group delay and superluminal propagation: An electronic circuit approach," *IEEE J. Sel. Top. Quantum Electron.*, vol. 9, no. 1, pp. 43–51, Jan. 2003.
[3] H. Choi, Y. Jeong, C. D. Kim, and J. S. Kenney, "Efficiency enhancement of feedforward amplifiers by employing a negative group delay circuit," *IEEE Trans. Microw. Theory Techn.*, vol. 58, no. 5, pp. 1116–1125, May 2010.
[4] H. Choi, Y. Jeong, C. D. Kim, and J. S. Kenney, "Bandwidth enhancement of an analog feedback amplifier by employing a negative group delay circuit," *Progr. Electromagn. Res.*, vol. 105, pp. 253–272, 2010.
[5] H. Noto, K. Yamauchi, M. Nakayama, and Y. Isota, "Negative group delay circuit for feed-forward amplifier," in *IEEE MTT-S Int. Microw. Symp. Dig.*, Jun. 2007, pp. 1103–1106.
[6] B. Ravelo, M. L. Roy, and A. Perennec, "Application of negative group delay active circuits to the design of broadband and constant phase shifters," *Microw. Opt. Technol. Lett.*, vol. 50, no. 12, pp. 3078–3080, Dec. 2008.
[7] S. S. Oh and L. Shafai, "Compensated circuit with characteristics of lossless double negative materials and its application to array antennas," *IET Microw. Antennas Propag.*, vol. 1, no. 1, pp. 29–38, Feb. 2007.
[8] D. Solli and R. Y. Chiao, "Superluminal effects and negative delays in electronics, and their application," *Phys. Rev. E, Stat. Phys. Plasmas Fluids Relat. Interdiscip. Top.*, no. 5, pp. 056601 1–0566101 4, Nov. 2002.
[9] Y. Jeong, H. Choi, and C. D. Kim, "Experimental verification for time advancement of negative group delay in RF electronics circuits," *Electron. Lett.*, vol. 46, no. 4, pp. 306–307, Feb. 2010.
[10] S. Lucyszyn, I. D. Robertson, and A. H. Aghvami, "Negative group delay synthesizer," *Electron. Lett.*, vol. 29, no. 9, pp. 798–800, Apr. 1993.
[11] S. Lucyszyn and I. D. Robertson, "Analog reflection topology building blocks for adaptive microwave signal processing applications," *IEEE Trans. Microw. Theory Techn.*, vol. 43, no. 3, pp. 601–611, Mar. 1995.
[12] B. Ravelo, A. Perennec, M. L. Roy, and Y. G. Boucher, "Active microwave circuit with negative group delay," *IEEE Microw. Wireless Compon. Lett.*, vol. 17, no. 12, pp. 861–863, Dec. 2007.
[13] H. Choi, K. Song, C. D. Kim, and Y. Jeong, "Synthesis of negative group delay time circuit," in *Proc. Asia–Pacific Microw. Conf.*, 2008, pp. 1–4.
[14] H. Choi, Y. Kim, Y. Jeong, and C. D. Kim, "Synthesis of reflection type negative group delay circuit using transmission line resonator," in *Proc. 39th Eur. Microw. Conf.*, Sep. 2009, pp. 902–605.
[15] C. D. Broomfield and J. K. A. Everard, "Broadband negative group delay networks for compensation of microwave oscillators and filters," *Electron. Lett.*, vol. 9, no. 23, pp. 1931–1932, Nov. 2000.
[16] M. Kandic and G. E. Bridges, "Bilateral gain-compensated negative group delay circuit," *IEEE Microw. Wireless Compon. Lett.*, vol. 21, no. 6, pp. 308–310, Jun. 2011.
[17] B. Ravelo, A. Perennec, and M. Le. Roy, "Synthesis of broadband negative group delay active circuits," in *IEEE MTT-S Int. Microw. Symp. Dig.*, Jun. 2007, pp. 2177–2180.
[18] H. Choi, Y. Kim, Y. Jeong, and J. Lim, "A design of size-reduced negative group delay circuit using a stepped impedance resonator," in *Proc. Asia–Pacific Microw. Conf.*, Dec. 2010, pp. 118–1121.
[19] M. Kandic and G. E. Bridges, "Asymptotic limit of negative group delay in active resonator-based distributed circuits," *IEEE Trans. Circuit System I, Reg. Papers*, vol. 58, no. 8, pp. 1727–1735, Aug. 2011.
[20] H. Choi, G. Chaudhary, T. Moon, Y. Jeong, J. Lim, and C. D. Kim, "A design of composite negative group delay circuit with lower signal attenuation for performance improvement of power amplifier linearization techniques," in *IEEE MTT-S Int. Microw. Symp. Dig.*, Jun. 2011, pp. 1–4.
[21] O. F. Sidhiqui, M. Mojahedi, and G. V. Eleftheriades, "Periodically loaded transmission line with effective negative group delay index and negative group velocity," *IEEE Trans. Antenna Propag.*, vol. 51, no. 10, pp. 2619–2625, Oct. 2010.
[22] Y. C. Ou and G. M. Rebeiz, "Lumped element fully tunable bandstop filters for cognitive radio applications," *IEEE Trans. Microw. Theory Techn.*, vol. 59, no. 10, pp. 2461–2468, Oct. 2011.
[23] M. Y. Hsieh and S. M. Wang, "Compact and wideband microstrip bandstop filter," *IEEE Microw. Wireless Compon. Lett.*, vol. 15, no. 7, pp. 472–474, Jul. 2005.
[24] M. K. Mandal, K. Divyabramham, and S. Sanyal, "Compact, wideband bandstop filters with sharp rejection characteristics," *IEEE Microw. Wireless Compon. Lett.*, vol. 18, no. 10, pp. 665–667, Oct. 2006.

[25] I. Shapir, "An improved narrowband microwave bandstop filter," in *Proc. Eur. Microw. Conf.*, 1998, pp. 210–214.
[26] S. Amari and U. Rosenberg, "Direct synthesis of a new class of bandstop filters," *IEEE Trans. Microw. Theory Techn.*, vol. 52, no. 2, pp. 607–616, Feb. 2004.
[27] I. C. Hunter, *Theory and Design of Microwave Filter*, ser. Electromagn. Waves. Stevenage, U.K.: IET, 2006.
[28] G. Mathaei, L. Young, and E. M. T. Jones, *Microwave Filters: Impedance Matching Networks and Coupling Structures*. Dedham, MA, USA: Artech. House, 1964.

Girdhari Chaudhary (S'10–M'13) received the B.E. degree in electronics and communication engineering from Nepal Engineering College (NEC), Kathmandu, Nepal, in 2004, the M.Tech. degree in electronics and communication engineering from the Malaviya National Institute of Technology (MNIT), Jaipur, India, in 2007, and the Ph.D. degree in electronics engineering from Chonbuk National University, Jollabuk-do, Korea, in 2013.

He is currently a Post-Doctoral Researcher with HOPE-IT Human Resource Development Center–BK21 PLUS, Division of Electronics Engineering, Chonbuk National University. He has authored or coauthored over 30 papers in international journals and conference proceedings. His research interests include multi-band tunable passive circuits, NGD circuits and their applications, and high-efficiency power amplifiers.

Yongchae Jeong (M'99–SM'10) received the BSEE, MSEE, and Ph.D. degrees in electronics engineering from Sogang University, Seoul, Korea, in 1989, 1991, and 1996, respectively.

From 1991 to 1998, he was a Senior Engineer with Samsung Electronics. In 1998, he joined the Division of Electronics Engineering, Chonbuk National University, Jollabuk-do, Korea. From July 2006 to December 2007, he was with the Georgia Institute of Technology, as a Visiting Professor. He is currently a Professor, Member of the Information Technology (IT) Convergence Research Center, and Director of the HOPE-IT Human Resource Development Center of BK21 PLUS, Chonbuk National University. He currently teaches and conducts research in the area of microwave passive and active circuits, mobile and satellite base-station RF systems, design of periodic defected transmission lines, and RF integrated circuit (RFIC) design. He has authored or coauthored over 100 papers in international journals and conference proceedings.

Dr. Jeong is a member of the Korea Institute of Electromagnetic Engineering and Science (KIEES).

Jongsik Lim (S'90–M'93–SM'05) received the BSEE and MSEE degrees in electronic engineering from Sogang University, Seoul, Korea, in 1991 and 1993, respectively, and the Ph.D. degree from the School of Electrical Engineering and Computer Science, Seoul National University, Seoul, Korea, in 2003.

In 1993, he joined ETRI, Daejeon, Korea, where, for six years, he was with the Satellite Communication Division, as a Senior Member. He was one of the key members in the development of monolithic microwave integrated circuit (MMIC) low-noise amplifiers (LNAs) and solid-state power amplifiers (SSPAs) for ETRI 20/30-GHz satellite transponders. From March to July 2003, he was with the Division of Information Technology, Brain Korea 21 Project, Seoul National University, as a Post Doctoral Fellow, and gave lectures in the graduate schools of Soonchunhyang University and Soongsil University. From July 2003 to September 2004, he was a Patent Examiner with the Korean Intellectual Property Office (KIPO). In September 2004, he rejoined ETRI, as a Senior Research Member of the Antenna Technology Research Team/Radio Technology Group. Since March 2005, he has been with the Department of Electrical Engineering, Soonchunhyang University, Chungcheongnam-do, Korea, as a member of the faculty. His current research interests include the design of passive and active circuits for RF/microwave and millimeter waves with microwave integrated circuit (MIC)/MMIC technology, modeling of active devices, design of high power amplifiers for mobile communications, applications of periodic structures to RF/microwave circuits, and modeling of passive structures having periodic structures.

Dr. Lim is a member of the Institute of Electronics, Information and Communication Engineers (IEICE), Japan, and Korea Institute of Electromagnetic Engineering and Science (KIEES).